Mass Mapping Sites of Nitration in Tyrosine Hydroxylase: Random vs Selective Nitration of Three Tyrosine Residues

ARTICLE *in* CHEMICAL RESEARCH IN TOXICOLOGY · MAY 2003

Impact Factor: 3.53 · DOI: 10.1021/tx0256681 · Source: PubMed

3 AUTHORS, INCLUDING:

Donald Kuhn
Wayne State University
163 PUBLICATIONS **5,080** CITATIONS

SEE PROFILE

Mass Mapping Sites of Nitration in Tyrosine Hydroxylase: Random vs Selective Nitration of Three Tyrosine Residues

Chad R. Borges,[†] Donald M. Kuhn,[‡,§,||] and J. Throck Watson*[,†]

Department of Biochemistry, Michigan State University, East Lansing, Michigan 48824, Department of Psychiatry and Behavioral Neurosciences and Center for Molecular Medicine and Genetics, Wayne State University School of Medicine, Detroit, Michigan 48201, and John D. Dingell VA Medical Center, Detroit, Michigan 48201

Received November 27, 2002

Previous work has shown that tyrosine residues Y423, Y428, and Y432 are potential targets for nitration when tyrosine hydroxylase is exposed to peroxynitrite. For any given protein molecule, up to three nitration events involving these residues may occur. In an effort to determine whether this nitration is directed toward a particular tyrosine residue or randomly distributed among all three tyrosine residues, the goal of this study was to determine whether a singly nitrated molecule was always nitrated at a particular tyrosine residue or whether the initial nitration event was randomly distributed among all three tyrosine residues. Isolation of the singly nitrated peptide V410-E436, followed by subsequent cleavage at D425 and analysis of the resulting peptide fragments by matrix-assisted laser desorption ionization mass spectrometry and LC/MS/MS revealed that the first nitration event was randomly distributed among Y423, Y428, and Y432.

Introduction

Tyrosine residue nitration within proteins serves as an indicator of toxic insult (*1*−*5*) and plays roles in signal transduction (*5*, *6*). The mechanisms of tyrosine nitration probably involve multiple chemical pathways (*5*, *7*−*9*) in different cases and have yet to be completely elucidated.

In the course of investigating tyrosine nitration events within tyrosine hydroxylase (TH) (*10*), the question arose as to whether complete nitration is accomplished as a directed, sequential series of events. That is, could it be that one tyrosine residue is more susceptible to attack by peroxynitrite-related species than the other two and therefore always becomes nitrated before the others? On the other hand, because peroxynitrite-mediated nitration is not an enzyme-mediated process (*7*, *11*, *12*) (except, perhaps, in rare cases (*13*, *14*)), nitration events should be equally distributed among solvent-exposed tyrosine residues. Heretofore, no evidence for either case has been presented.

We have shown previously that three tyrosine residues within TH are targets of nitration, with up to three nitration events per TH molecule. (For further information on the nitration status of other tyrosine residues within this protein, readers are directed to Kuhn et al. (*10*). The crystal structure of rat TH is available from the Protein Data Bank as 1TOH.) Here, we have pursued the question of whether a singly nitrated TH molecule is always nitrated at a particular tyrosine residue or whether the nitration event is equally distributed among the three affected tyrosine residues.

Materials and Methods

Materials. Glu-C (V8 protease) endoproteinase was obtained from Roche Applied Science (Indianapolis, IN). Asp-N endoproteinase was purchased from Sigma (St. Louis, MO). Following expression as previously described (*15*, *16*), TH was treated with 500 μM peroxynitrite as previously explained (*10*). All other materials were of the highest purity commercially available.

Isolation of a Singly Nitrated Peptide Containing Y423, Y428, and Y432. A 130 μg amount of peroxynitrite-treated TH (TH−$ONOO^-$) was purified by reversed-phase HPLC. The HPLC system consisted of a Waters Alliance 2695 separations module connected to a Waters 2487 dual wavelength absorbance detector set at 214 nm. A gradient of 20−65% acetonitrile in 0.1% trifluoroacetic acid (TFA) (in house-distilled water[1]) was applied in a 60 min time period over a Vydac C18 (4.6 mm × 250 mm, 5 μm particle size, 300 Å pores) column. Fractions corresponding to the whole protein were collected and dried in a vacuum system. TH−$ONOO^-$ was reconstituted in 60 μL of 6 M guanidine hydrochloride in 50 mM trizma hydrochloride buffer, pH 8.0. To this were added 330 μL of water and 330 μL of 1 mM $CaCl_2$ in 50 mM trizma hydrochloride, pH 7.6. Three micrograms of Glu-C endoproteinase (in 3 μL) was added to each sample, which was mixed and allowed to sit for 18 h at room temperature. The Glu-C digest was separated by microbore HPLC (on the above system) with the flow rate set at 0.05 mL/

* To whom correspondence should be addressed. Tel: 517-353-0855. Fax: 517-353-9334. E-mail: watsonj@msu.edu.
[†] Michigan State University.
[‡] Department of Psychiatry and Behavioral Neurosciences, Wayne State University School of Medicine.
[§] Center for Molecular Medicine and Genetics, Wayne State University School of Medicine.
[||] John D. Dingell VA Medical Center.

[1] House-distilled water was not used for the peroxynitrite labeling portions of the work, which was done at a different laboratory (using MilliQ grade 18.2 MΩ cm deionized water) than the HPLC and mass spectrometric analyses. House-distilled water was used because the author performing the HPLC and mass spectrometric analysis was, at the time, not aware of other available sources of pure water.

10.1021/tx0256681 CCC: $25.00
Published on Web 03/19/2003

min across a 150 mm × 1.0 mm column with the same sorbent as above. Solvent A was 0.1% TFA in house-distilled water containing 10 μm EDTA-free acid. Solvent B was 0.1% TFA in 98:2 acetonitrile/house-distilled water containing 10 μm EDTA-free acid. A gradient of 0% B to 45% B was applied linearly over 60 min, followed by ramping to 65% B over another 10 min, and finally ramping to 95% B over an additional 5 min. Eluting peptides were monitored by absorbance at 214 and 350 nm. The chromatogram produced by monitoring absorbance at 350 nm indicated the presence of nitrotyrosine-containing peptides (*17*) and allowed for collection of fractions containing such peptides. From prior experience (*10*), it was known that a proteolytic peptide was produced by Glu-C cleavage at E409 and E436 (V410-E436), containing Y423, Y428, and Y432. The V410-E436 fragment was present in four forms: unmodified, singly nitrated, doubly nitrated, and triply nitrated. Each form was chromatographically separated from the others and individually collected.

Cleavage of Singly Nitrated V410-E436 by Asp-N. The fraction containing singly nitrated V410-E436 was dried under vacuum and reconstituted in 15 μL of 6 M guanidine HCl/50 mM Tris HCl buffer, pH 8.0, 115 μL of 0.1 M ammonium bicarbonate buffer, pH 8.5, and 50 μL of 10 mM Tris HCl, pH 8.0, containing 2 μg of Asp-N endoproteinase. Digestion proceeded for 18 h at 37 °C. Asp-N cleavage products of V410-E436 were then chromatographically separated by microbore RP-HPLC as described above. Fractions containing peptides that produced an absorbance peak at 350 nm were collected, dried, and reconstituted in 6 μL of 50/50 acetonitrile/0.1% TFA. An aliquot of 0.75 μL from each fraction was removed and mixed with an equal volume of 50/50 acetonitrile/0.1% TFA solution that had been saturated with α-cyano-4-hydroxycinnamic acid (CHCA) for subsequent analysis by matrix-assisted laser desorption ionization mass spectrometry (MALDI-MS).

Analysis of Asp-N Cleavage Products by MALDI-MS. Samples were prepared by spotting 0.5 μL analyte + matrix onto a gold-plated well-less sample plate with CHCA as the matrix using the modified thin-layer technique of Cadene and Chait (*18*). MALDI mass spectra were acquired on a Voyager DE-STR time-of-flight (TOF) mass spectrometer (Perkin-Elmer Biosystems Inc., Framingham, MA) equipped with a 337 nm nitrogen laser. Measurements were made in linear mode with the accelerating voltage set to 20 000 V, grid voltage at 95%, guide wire at 0.05%, and extraction delay time at 150 ns. TOF to mass conversion was achieved with the use of external standards of bradykinin (monoisotopic calculated mass for MH^+ = 1060.57 Da; average mass for MH^+ = 1061.22 Da) and bovine pancreatic insulin (average calculated mass for MH^+ = 5734.56 Da; average calculated mass-to-charge ratio for $[M + 2H]^{2+}$ = 2867.78).

Analysis of Asp-N Cleavage Products by LC/MS/MS. LC/MS/MS analysis was carried out on a Waters CapLC system connected to a ThermoFinnigan LCQ Deca ion trap mass spectrometer equipped with a nanoelectrospray ion source. A 1−4 μL aliquot of each fraction collected following Asp-N cleavage of V410-E436 was diluted to 7 μL and a final composition of 4%/96% (v/v) acetonitrile/0.1% TFA. Three microliters from each sample were injected onto a Peptide CapTrap (Michrom Bioresources) and washed for 6 min at 20 μL/min with 98%/2% deionized water/ACN containing 0.1% formic acid. The divert valve was then switched to flow over the CapTrap, through a titanium tee union connecting the fused silica column (and where a 1.7 kV spray voltage was applied to the mobile phase) and then through a 75 μm × 5 cm ProteoPep C18 PicoFrit column with a 15 μm ID tip (New Objective, Woburn, MA) at approximately 250 nL/min at a gradient ramped to 50% ACN over 10 min. Data were acquired by the mass spectrometer in "triple play" mode performing a full scan from 300 to 2000 *m/z* followed by a Zoomscan of the most abundant ion (to determine charge state) and then an MS/MS scan of the products of the isolated ion (2.0 *m/z* isolation width) at 35% normalized collision energy.

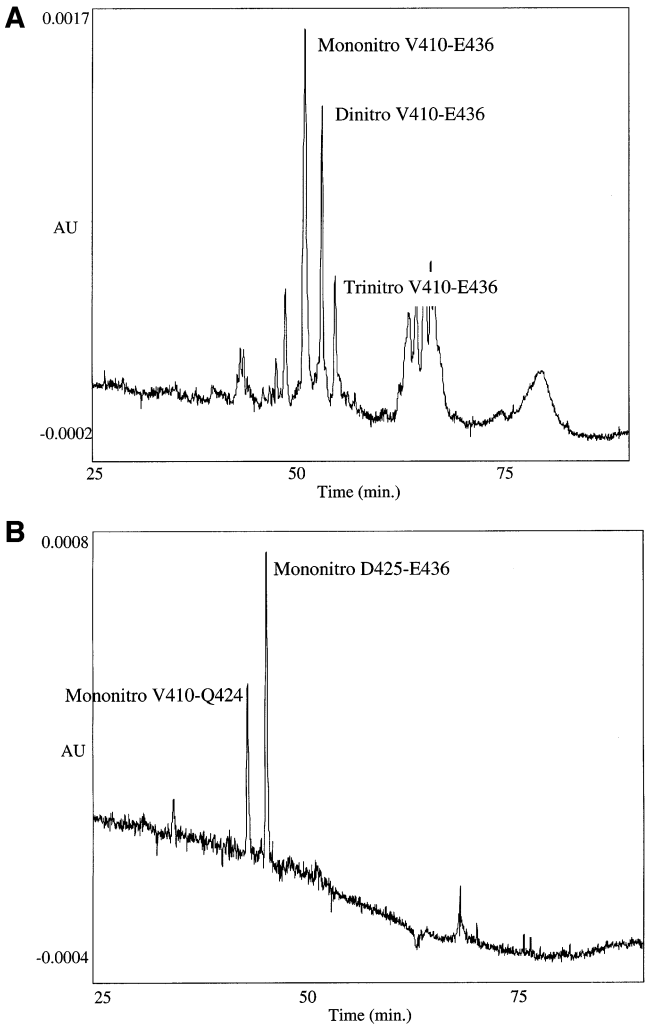

Figure 1. HPLC with detection by absorbance at 350 nm of (A) Glu-C-cleaved TH−$ONOO^-$, where the most intense peak (at ∼51 min) represents mononitro-V410-E436 and (B) Asp-N-cleaved mononitro-V410-E436.

Results and Discussion

Singly, doubly, and triply nitrated forms of the peptide V410-E436, produced by Glu-C-mediated cleavage of TH−$ONOO^-$, were separated by microbore RP-HPLC (Figure 1A). (On the basis of peak area from HPLC absorbance at 214 nm, the majority of the V410-E436 peptide appears to have been in the unmodified form.) The most intense peak, in Figure 1A, at ∼51 min represents mononitrated V410-E436, and the two peaks immediately following represent dinitrated and trinitrated V410-E436, respectively. Other peaks most likely represent differentially cleaved peptides containing nitrotyrosine residue(s); they were, however, not identified. Analysis of the collected fractions by MALDI-MS indicated that the fraction corresponding to singly nitrated V410-E436 contained only a small amount of unnitrated V410-E436 and no doubly nitrated species. Following proteolytic cleavage of singly nitrated V410-E436 by Asp-N at D425, the digest mixture was analyzed by RP-HPLC, producing two peaks in the 350 nm chromatogram (Figure 1B). Fractions corresponding to these peaks were collected. On the basis of peak height, the later eluting peptide was approximately twice as abundant as the earlier eluting peptide. Analysis of the first fraction by MALDI-MS indicated the presence of singly nitrated

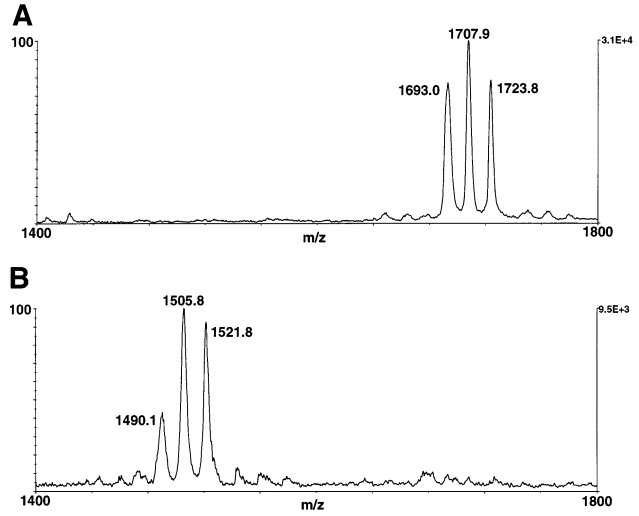

Figure 2. Analysis by MALDI-MS of chromatographically separated Asp-N cleavage products of V410-E436 resulting in (A) mononitro-V410-Q424, calculated average MH^+ mass = 1723.9 Da, and (B) mononitro-D425-E436, calculated average MH^+ mass = 1521.6 Da. Spectra were smoothed after acquisition.

V410-Q424 (H_2N-VRAFDPDTAAVQPY$_{NO_2}$Q−*COOH*) as represented by a peak at *m/z* 1723.8 (Figure 2A) (calculated average MH^+ mass = 1723.9 Da). Prompt fragmentation of the ion represented by this peak occurred, involving consecutive losses of 16 and/or 15 Da, which helped to confirm the presence of the nitrotyrosine moiety (*19*). Thus, Y423 was, at least in some TH molecules, nitrated before either Y428 or Y432. Analysis of the second, later eluting fraction (Figure 1B) by MALDI-MS initially produced a set of peaks consistent with a copper adduct of nitrated D425-E436, that is, $[M_{NO_2} + Cu]^+$. Treatment of this fraction with 200 μM bicinchoninic acid (a copper(I) ion chelator) and reanalysis by MALDI-MS produced a set of peaks with the largest at *m/z* 1521.8 (Figure 2B), representing the nitrated MH^+ ion of D425-E436 (calculated average MH^+ mass = 1521.6 Da). These results indicated that for protein molecules that had been singly nitrated between V410-E436, the nitration event was distributed between Y423 and Y428 and/or Y432. Because nitration was detected on both V410-Q424 and D425-E436—peptides that had originated from singly nitrated V410−436—unnitrated forms of these peptides must have been produced following digestion of V410-E436 by Asp-N. No unnitrated forms of V410-Q424 or D425-E436 were detected by MALDI-MS in the same chromatographic fractions as the nitrated forms, however, presumably because they were chromatographically separated from the nitrated forms and not collected along with them. Peaks in the 214 nm absorbance chromatogram representing unnitrated forms of these peptides were not readily identified due to the presence of autolytic products of Asp-N (data not shown), but analysis of an earlier eluting fraction by MALDI-MS demonstrated the presence of the unnitrated forms of these peptides. Together with the HPLC data suggesting an approximately 1:2 nitrotyrosine ratio of V410-Q424:D425-E436, these data strongly suggested that the single nitration event was distributed equally among all three tyrosine residues in question; however, the possibility remained that the first nitration event was distributed between only Y423 and Y428 or between only Y423 and Y432 with the second tyrosine residue nitrated twice as frequently as Y423.

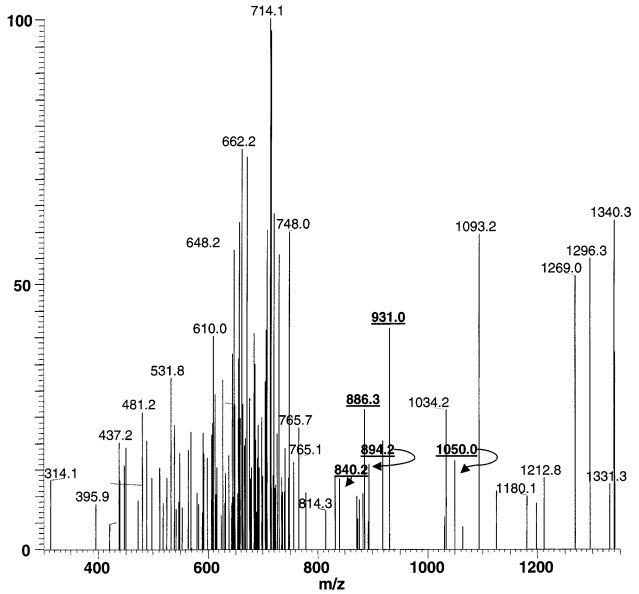

Figure 3. MS/MS spectrum (average of two scans) of the ions produced when D425-E436, in the form of $[M + Fe^{3+} - H]^{2+}$ at *m/z* 787.2, was subjected to CID. See Table 1 for peak assignments that elucidate the position of the nitrotyrosine residue within each precursor ion that produced the particular fragment ion corresponding to the assigned peak. These data indicate that in some D425-E436 molecules, the nitration event was at Y428, while in other molecules it was at Y432.

To further elucidate the distribution of tyrosine nitration, the peptide containing residues D425-E436 was subjected to LC/MS/MS analysis. A singly charged peptide with a monoisotopic mass of 1520.5 Da (calculated monoisotopic mass = 1520.7 Da), corresponding to mononitro-D425-E436, was isolated and subjected to collision-induced dissociation (CID) and subsequent MS^2 analysis but produced no detectable ions above the minimum detectable threshold at *m/z* 405. Interestingly, the base peak of the full scan mass spectrum of the chromatographic component of interest was at *m/z* 787.2, which represents a doubly charged $[M + Fe^{3+} - H]^{2+}$ ion. A peak at *m/z* 1573.2 representing $[M + Fe^{3+} - 2H]^+$ at about 15% relative intensity was also found. (As it was subsequently determined, iron (Fe^{3+}) and the aforementioned copper (Cu^+) came from the house-distilled water used for HPLC separation of proteolytic peptides.) Repeated CID and analysis by MS^2 of the ion represented by the peak at *m/z* 787.2 consistently produced MS^2 spectra containing many peaks (Figure 3 and Table 1). (Analysis of the MH^+ ion at *m/z* 1520.5 by CID and subsequent MS^2 scan produced no ion current in the *m/z* 405−1535 range.) To provide information on which tyrosine was nitrated in any given molecule, the peptide had to fragment between Y428 and Y432. Most of the peaks in the MS^2 spectrum do not arise from such fragmentations. As highlighted in Figure 3, however, peaks at *m/z* 840.2, *m/z* 886.3, *m/z* 894.2, *m/z* 931.0, and *m/z* 1050.0 represent such fragmentation reactions and show that in some of the precursor ions Y428 was nitrated, while in other precursor ions Y432 was nitrated. Overall, the results described here indicate a random distribution of the first nitration event among Y423, Y428, and Y432.

In most cases, the $[M + Fe^{3+} - H]^{2+}$-derived fragment ions, including those represented by unassigned peaks

Table 1. Peak Assignments for Figure 3[a]

observed *m/z*	peak assignment	calculated *m/z*	indicates nitration at Tyr residue
662.2	$[b_{10} + Fe - NH_3 - H]^{2+}$ or $[b_{10} + Fe - NH_3 - 2H]^{2+}$	662.3 or 661.8	NI
670.7	$[b_{10} + Fe - H]^{2+}$ or $[b_{10} + Fe - 2H]^{2+}$	670.8 or 670.3	NI
714.1	$[b_{11} + Fe - 2H]^{2+}$	713.8	NI
814.3	$[b6 + Fe - H_2O - 2H]+$ or $[b7 - H_2O]+$	814.3 or 814.4	?
832.2	$[b_6 + Fe - 2H]^+$ or b_7^+	832.3 or 832.4	?
840.2	$\mathbf{y_7}^+$	**840.4**	**Y428**
886.3	$\mathbf{[b_7 + Fe - 2H]}^+$	**886.4**	**Y432**
894.2	$\mathbf{[y_7 + Fe - 2H]}^+$	**894.4**	**Y428**
931.0	$\mathbf{[b_7 + Fe - 2H]}^+$	**931.4**	**Y428**
1034.2	$[b_8 + Fe - CO_2 - NH_3 - 2H]^+$	1033.4	NI
1050.0	$\mathbf{[y_8 + Fe - NH_3 - 2H]}^+$	**1050.4**	**Y432**
1093.2	$[b_8 + Fe - 3H]^+$	1093.4	NI
1180.1	$[b_9 + Fe - CO_2 - NH_3 - 2H]^+$	1180.5	NI
1197.4	$[b_9 + Fe - CO_2 - 2H]^+$	1197.5	NI
1212.8	$[y_9 + Fe - H_2O - 2H]^+$	1212.5	NI
1269.0	$[b_{10} - NH_3]^+$ or $[b_{10} - H_2O]^+$	1269.5 or 1268.6	NI
1296.3	$[b_{10} + Fe - CO_2 - 2H]^+$ or $[y_{10} + Fe - H_2O - NH_3 - 2H]^+$	1296.6 or 1296.5	NI
1331.3	$[y_{10} + Fe - 2H]^+$	1331.6	NI
1340.3	$[b_{10} + Fe - 2H]^+$	1340.6	NI

[a] Assignments that provide information on the position of the nitrotyrosine residue within the precursor ion are in bold. Sequence of D425-E436: H_2N−DQTYQPVYFVSE−COOH. NI indicates that the assigned ion does not provide any information as to the location of the nitrotyrosine residue within the peptide. The question mark indicates that one possible assignment indicates nitration at Y428 while the other possible assignment indicates nitration at Y432; mass accuracy is not good enough to distinguish between the two possible assignments.

in Figure 3, retained the iron atom, producing $[\mathbf{b_n/y_n} + Fe - 2H]^+$ ions. Retention of metal cations by peptide fragment ions following CID is well-documented (*20*−*23*). The unique feature of these ions, however, is that the iron atom appears to have been reduced during CID. To illustrate, the calculated mass for $[\mathbf{b_7}^+ + Fe^{2+} - 2H]^+$ ions matches the observed mass value within 0.1 Da. Without reduction of the iron atom, the assignment could be written as $[\mathbf{b_7} + Fe^{3+} - 2H]^+$, but a **b** ion can only become neutral through the loss of a proton from the cyclic oxazolonium moiety or, in the case of uncyclized species, through one electron reduction of the acylium cation to a neutral, less stable radical—an energetically unfavorable event. (A **y** ion must lose a proton to attain neutrality.) The peak assignments in Table 1 are written with the redox ambiguous formula $[\mathbf{b_n/y_n} + Fe - 2H]^+$, but the former scenario where an extra proton is lost creates a $[\mathbf{b_7} + Fe^{3+} - 3H]^+$ ion with a mass 1 Da lower than the observed mass, making the $[\mathbf{b_7}^+ + Fe^{2+} - 2H]^+$ ion, with a reduced iron atom, the best assignment for the observed peak. Prior to these observations, a precedent for reduction of metal cations by peptides following molecular excitation has been established (*24*, *25*).

These studies demonstrate the random distribution of an initial nitration event among three tyrosine residues of TH following a bolus addition of peroxynitrite to a final concentration of 500 μM[2]—a high, but not uncommonly high (*17*, *28*−*31*), peroxynitrite concentration. If the reactions generating nitrotyrosine were enzymatically mediated, it is conceivable that this concentration of peroxynitrite could bias the results in favor of nonselective tyrosine nitration. However, because tyrosine nitration by peroxynitrite is not enzymatically mediated (*7*, *11*, *12*) (except, perhaps, in rare cases (*13*, *14*)) but most likely occurs (in the presence of CO_2) via attack of a $^{\bullet}NO_2$ radical on a tyrosyl radical generated by $CO_3^{\bullet-}$ (where the $^{\bullet}NO_2$ and $CO_3^{\bullet-}$ radicals are derived from the homolytic cleavage of nitrosoperoxycarbonate, ONOO−CO_2^-) (*7*, *11*, *12*), the rates of reaction would simply depend on the concentrations of these two radicals and the "available" concentration of the tyrosine residue in question. (Availability depends on tyrosine residue microenvironment within the protein.) Because this nonenzymatic reaction mechanism governs all three tyrosine residues (meaning the reaction rate law would be the same for all three reactions), a decrease in the concentration of peroxynitrite would not generate a disproportionate yield of nitration at one particular nitrotyrosine residue relative to the yield at the other nitrotyrosine residues. (This would only be suspected if nitration was enzymatically mediated, i.e., controlled by K_M and V_{max} values.) Because of insufficient yields, tyrosine-nitrated V410-E436 generated from lower concentrations of peroxynitrite was not examined in depth to determine random vs selective tyrosine nitration distribution.

[2] This concentration of peroxynitrite was needed to produce a large enough quantity of the mononitrated V410-E436 peptide for subsequent analysis. Undoubtedly, at pH 7.4, the concentration of $ONOO^-$/ONOOH decreased rapidly with time (*7*, *26*, *27*).

Conclusion

Isolation of singly nitrated V410-E436, followed by subsequent cleavage at D425 and analysis of the resulting peptide fragments by MALDI-MS and LC/MS/MS, revealed that the first nitration event is randomly distributed among Y423, Y428, and Y432.

Acknowledgment. This work was supported by NIH Grant GM60567, NIH NIDA Grant RO1 DA10756, and NIDA Grant K05 DA14692.

References

(1) Greenacre, S. A., and Ischiropoulos, H. (2001) Tyrosine nitration: localisation, quantification, consequences for protein function and signal transduction. *Free Radical Res.* **34**, 541−581.
(2) Ischiropoulos, H. (1998) Biological tyrosine nitration: a pathophysiological function of nitric oxide and reactive oxygen species. *Arch. Biochem. Biophys.* **356**, 1−11.
(3) van der Vliet, A., Eiserich, J. P., Kaur, H., Cross, C. E., and Halliwell, B. (1996) Nitrotyrosine as biomarker for reactive nitrogen species. *Methods Enzymol.* **269**, 175−184.
(4) Beckman, J. S., and Koppenol, W. H. (1996) Nitric oxide, superoxide, and peroxynitrite: the good, the bad, and ugly. *Am. J. Physiol.* **271**, C1424−C1437.

(5) Hanafy, K. A., Krumenacker, J. S., and Murad, F. (2001) NO, nitrotyrosine, and cyclic GMP in signal transduction. *Med. Sci. Monit.* **7**, 801−819.
(6) Maccarrone, M., Putti, S., and Finazzi Agro, A. (1997) Nitric oxide donors activate the cyclo-oxygenase and peroxidase activities of prostaglandin H synthase. *FEBS Lett.* **410**, 470−476.
(7) Squadrito, G. L., and Pryor, W. A. (2002) Mapping the Reaction of Peroxynitrite with CO(2): Energetics, Reactive Species, and Biological Implications. *Chem. Res. Toxicol.* **15**, 885−895.
(8) Gunther, M. R., Hsi, L. C., Curtis, J. F., Gierse, J. K., Marnett, L. J., Eling, T. E., and Mason, R. P. (1997) Nitric oxide trapping of the tyrosyl radical of prostaglandin H synthase-2 leads to tyrosine iminoxyl radical and nitrotyrosine formation. *J. Biol. Chem.* **272**, 17086−17090.
(9) Gunther, M. R., Sturgeon, B. E., and Mason, R. P. (2002) Nitric oxide trapping of the tyrosyl radical-chemistry and biochemistry. *Toxicology* **177**, 1−9.
(10) Kuhn, D. M., Sadidi, M., Lu, X., Kriepke, C., Geddes, T., Borges, C., and Watson, J. T. (2002) Peroxynitrite-induced nitration of tyrosine hydroxylase: identification of tyrosines 423, 428, and 432 as sites of modification by MALDI-TOF mass spectrometry and tyrosine-scanning mutagenesis. *J. Biol. Chem.* **7**, 7.
(11) Santos, C. X., Bonini, M. G., and Augusto, O. (2000) Role of the carbonate radical anion in tyrosine nitration and hydroxylation by peroxynitrite. *Arch. Biochem. Biophys.* **377**, 146−152.
(12) Augusto, O., Bonini, M. G., Amanso, A. M., Linares, E., Santos, C. C., and De Menezes, S. L. (2002) Nitrogen dioxide and carbonate radical anion: two emerging radicals in biology. *Free Radical Biol. Med.* **32**, 841−859.
(13) Beckman, J. S., Ischiropoulos, H., Zhu, L., van der Woerd, M., Smith, C., Chen, J., Harrison, J., Martin, J. C., and Tsai, M. (1992) Kinetics of superoxide dismutase- and iron-catalyzed nitration of phenolics by peroxynitrite. *Arch. Biochem. Biophys.* **298**, 438−445.
(14) Ischiropoulos, H., Zhu, L., Chen, J., Tsai, M., Martin, J. C., Smith, C. D., and Beckman, J. S. (1992) Peroxynitrite-mediated tyrosine nitration catalyzed by superoxide dismutase. *Arch. Biochem. Biophys.* **298**, 431−437.
(15) Kuhn, D. M., Aretha, C. W., and Geddes, T. J. (1999) Peroxynitrite inactivation of tyrosine hydroxylase: mediation by sulfhydryl oxidation, not tyrosine nitration. *J. Neurosci.* **19**, 10289−10294.
(16) Kuhn, D. M., Arthur, R. E., Jr., Thomas, D. M., and Elferink, L. A. (1999) Tyrosine hydroxylase is inactivated by catechol-quinones and converted to a redox-cycling quinoprotein: possible relevance to Parkinson's disease. *J. Neurochem.* **73**, 1309−1317.
(17) Guittet, O., Decottignies, P., Serani, L., Henry, Y., Le Marechal, P., Laprevote, O., and Lepoivre, M. (2000) Peroxynitrite-mediated nitration of the stable free radical tyrosine residue of the ribonucleotide reductase small subunit. *Biochemistry* **39**, 4640−4648.
(18) Cadene, M., and Chait, B. T. (2000) A robust, detergent-friendly method for mass spectrometric analysis of integral membrane proteins. *Anal. Chem.* **72**, 5655−5658.
(19) Sarver, A., Scheffler, N. K., Shetlar, M. D., and Gibson, B. W. (2001) Analysis of peptides and proteins containing nitrotyrosine by matrix- assisted laser desorption/ionization mass spectrometry. *J. Am. Soc. Mass Spectrom.* **12**, 439−448.
(20) Loo, J. A., Hu, P., and Smith, R. D. (1994) Interaction of angiotensin peptides and zinc metal ions probed by electrospray ionization mass spectrometry. *J. Am. Soc. Mass Spectrom.* **5**, 959−965.
(21) Hu, P., Sorensen, C., and Gross, M. L. (1995) Influences of peptide side chains on the metal ion binding site in metal ion-cationized peptides: participation of aromatic rings in metal chelation. *J. Am. Soc. Mass Spectrom.* **6**, 1079−1085.
(22) Nemirovskiy, O. V., and Gross, M. L. (1996) Complexes of iron-(II) with cysteine-containing peptides in the gas phase. *J. Am. Soc. Mass Spectrom.* **7**, 977−980.
(23) Nemirovskiy, O. V., and Gross, M. L. (1998) Gas-phase studies of the interactions of Fe2+ with cysteine-containing peptides. *J. Am. Soc. Mass Spectrom.* **9**, 1285−1292.
(24) Lavanant, H., Virelizier, H., and Hoppilliard, Y. (1998) Reduction of copper(II) complexes by electron capture in an electrospray ionization source. *J. Am. Soc. Mass Spectrom.* **9**, 1217−1221.
(25) Barbeau, K., Rue, E. L., Bruland, K. W., and Butler, A. (2001) Photochemical cycling of iron in the surface ocean mediated by microbial iron(III)-binding ligands. *Nature* **413**, 409−413.
(26) Lymar, S. V., and Hurst, J. K. (1995) Rapid reaction between peroxonitrite ion and carbon dioxide: Implications for biological activity. *J. Am. Chem. Soc.* **117**, 8867−8868.
(27) Merenyi, G., and Lind, J. (1998) Free radical formation in the peroxynitrous acid (ONOOH)/peroxynitrite (ONOO-) system. *Chem. Res. Toxicol.* **11**, 243−246.
(28) MacMillan-Crow, L. A., Crow, J. P., and Thompson, J. A. (1998) Peroxynitrite-mediated inactivation of manganese superoxide dismutase involves nitration and oxidation of critical tyrosine residues. *Biochemistry* **37**, 1613−1622.
(29) Viner, R. I., Williams, T. D., and Schoneich, C. (1999) Peroxynitrite modification of protein thiols: oxidation, nitrosylation, and S-glutathiolation of functionally important cysteine residue(s) in the sarcoplasmic reticulum Ca-ATPase. *Biochemistry* **38**, 12408−12415.
(30) Blanchard-Fillion, B., Souza, J. M., Friel, T., Jiang, G. C., Vrana, K., Sharov, V., Barron, L., Schoneich, C., Quijano, C., Alvarez, B., Radi, R., Przedborski, S., Fernando, G. S., Horwitz, J., and Ischiropoulos, H. (2001) Nitration and inactivation of tyrosine hydroxylase by peroxynitrite. *J. Biol. Chem.* **276**, 46017−46023.
(31) Park, S. U., Ferrer, J. V., Javitch, J. A., and Kuhn, D. M. (2002) Peroxynitrite inactivates the human dopamine transporter by modification of cysteine 342: potential mechanism of neurotoxicity in dopamine neurons. *J. Neurosci.* **22**, 4399−4405.

TX0256681